Haploid mouse germ cell precursors from embryonic stem cells reveal *Xist* activation from a single X chromosome

Eishi Aizawa[1], Corinne Kaufmann[1], Sarah Sting[1], Remo Freimann[1], Anton Wutz[1,*]

[1]Institute of Molecular Health Sciences, Swiss Federal Institute of Technology, ETH Zurich, Zurich, Switzerland

*Correspondence: awutz@ethz.ch

Summary

Mammalian haploid cells have applications for genetic screening and substituting gametic genomes. Here we characterize a culture system for obtaining haploid primordial germ cell-like cells (PCGLCs) from haploid mouse embryonic stem cells (ESCs). We find that a haploid genome is maintained in PGCLCs with a high frequency indicating a substantially lower rate of diploidization than somatic cells. Characterization of the differentiating haploid ESCs reveals that *Xist* is activated from the single X chromosome. This observation suggests that X chromosome inactivation is initiated in haploid cells consistent with a model where autosomal blocking factors set a threshold for X-linked activators. The germline segregates from the epiblast and differs from somatic lineages in gene expression and epigenetic mechanisms. The ability of primordial germ cells for repressing *Xist* might contribute to the maintenance of a haploid genome.

23 # Introduction

24 In mice, the germline derives from cells of the proximal epiblast and primordial germ cells
25 (PGCs) segregate to an extraembryonic location adjacent to the posterior end of the
26 embryo. PGC differentiation has been recapitulated in cultures of mouse epiblast cells
27 (Ohinata et al., 2009). Furthermore, functional gametes have been obtained from primordial
28 germ cell-like cells (PGCLCs) derived from embryonic stem cells (ESCs) in mice (Hayashi
29 et al., 2012; Hayashi et al., 2011). Progress in culture techniques is opening opportunities
30 for studies of the mammalian germline (Hayashi and Saitou, 2013). Germ cells differ from
31 the somatic lineages in several key aspects including gene regulation and epigenetic
32 modification (Hill et al., 2018; Leitch et al., 2013). During migration to the genital ridges,
33 erasure of genomic imprinting occurs in PGCs, and the inactive X chromosome (Xi) is
34 reactivated in female PGCs (Sugimoto and Abe, 2007).

35 Mammalian dosage compensation is facilitated by inactivation of one of the two X
36 chromosomes in female cells (Lyon, 1961). Therefore, a single transcriptionally active X
37 chromosome (Xa) faces two sets of autosomes in the diploid genome. In mice, X
38 chromosome inactivation (XCI) is initiated by the long noncoding *Xist* RNA, which is
39 expressed from, and accumulates over the inactive X chromosome (Xi) before X-linked
40 gene repression (Galupa and Heard, 2018). *Xist* is first expressed in four-cell stage
41 blastomers and initiates imprinted XCI of the paternally inherited X chromosome (Okamoto
42 et al., 2004; Takagi and Sasaki, 1975). Cells that are destined to form the embryo reactivate
43 the Xi at the blastocyst stage. In the developing female epiblast two Xa are present before
44 embryonic day (E) 5.5, when random XCI is initiated (Mak et al., 2004). Thereafter, the Xi
45 is maintained in all somatic lineages, but in the female germline Xi reactivation is observed.

46 From E7.0 two Xa are present in PGCs (Ohhata and Wutz, 2013; Sugimoto and Abe, 2007).
47 These observations show the dynamics of the dosage compensation system.

48 The regulation of XCI remains to be fully understood. A number of observations
49 suggest that the X to autosome (X:A) ratio controls the initiation of XCI and *Xist* expression.
50 One model posits that autosomal blocking factors prevent *Xist* activation for explaining the
51 observation that a single X chromosome is insufficient for initiation of XCI in male cells
52 (Barakat et al., 2014; Kay et al., 1993; Pollex and Heard, 2019). In female cells, twice the
53 number of X-linked activators overcomes an activation threshold for *Xist* leading to the
54 initiation of XCI. Diffusible X-linked activators and autosomal blocking factors are beginning
55 to be understood (Barakat et al., 2014; Pollex and Heard, 2019). An alternative model is
56 based on the observation of paring of the X chromosomes at the X chromosome
57 inactivation center (*Xic*) (Bacher et al., 2006; Xu et al., 2007; Xu et al., 2006). The *Xic*
58 encompasses the *Xist* gene and other regulators of XCI including the antisense *Tsix*
59 transcript. Genetic elements that are required for *Xic* pairing have been identified and
60 shown to induce XCI when transgenically integrated into autosomes in male ESCs (Augui
61 et al., 2007). Furthermore, stochastic regulation of *Xist* has been proposed from studies of
62 tetraploid ESCs, where a variable number of X chromosomes displayed activation of *Xist*
63 upon entry into differentiation (Monkhorst et al., 2008). Investigating the X counting
64 mechanism in the context of different autosomal dosage has led to further understanding
65 of the underlying regulation.

66 The mechanism of XCI has been extensively studied in ESCs, as these recapitulate
67 the relevant developmental stages that would be difficult to access in the post-implantation
68 embryo. In mice, female ESCs initiate XCI at the entry into differentiation. With the

69 establishment of haploid ESCs (haESCs) the effect of ploidy on regulation of XCI can be
70 further studied. HaESCs are established from *in vitro* cultured haploid embryos (Elling et
71 al., 2011; Leeb and Wutz, 2011). HaESCs possess a haploid genome but also show a
72 tendency towards diploidization, which is strongly enhanced when haESCs enter
73 differentiation. Diploidization has, thus, far made studies of *Xist* activation difficult to
74 interpret as haploid cells are in the process of diploidization. Several factors that affect
75 diploidization have been extensively investigated in somatic lineage differentiation with the
76 aim to reduce the high rates of diploidization (Freimann and Wutz, 2017; He et al., 2018;
77 He et al., 2017; Olbrich et al., 2017; Olbrich et al., 2019; Takahashi et al., 2014). A previous
78 study has reported the germline competence of haESCs *in vivo* by blastocyst injection
79 (Leeb et al., 2012), but the ploidy of haESCs and their characterization during germ cell
80 differentiation have been less well studied.

81 Here, we report the successful differentiation of haESCs into haploid PGCLCs *in vitro*.
82 We show that a haploid genome is preferentially maintained in PGCLCs compared with
83 somatic cell lineages. We then use this system to investigate *Xist* activation in haploid cells.
84 Our data demonstrate that a single X chromosome is sufficient for *Xist* activation in a
85 haploid genome consistent with a lower threshold of autosomal blocking factors.

86

87 # Results

88 ## Differentiation of haESCs into haploid PGCLCs

89 To investigate the feasibility of germ cell differentiation from haESCs we followed a
90 previously established protocol (Hayashi et al., 2012; Hayashi et al., 2011). A mixed
91 population of haploid and diploid ESCs, containing 16.8% cells with a 1n DNA content

92 (G0/G1/S-phase haploid), were differentiated to epiblast-like cells (EpiLCs) for 2 days in
93 the presence of FGF2 and Activin A (Figure 1A, B). Subsequently, we aggregated the
94 EpiLCs for embryoid body (EB) formation. PGCLCs appeared between day 6 and 8 and
95 were identified by co-expression of the SSEA1 and integrin β3 surface markers. On day 7,
96 11.1% of the cells expressed both PGC markers (Figure 1C, D). Analysis of the ploidy
97 distribution by flow cytometry after DNA staining with Hoechst 33342 showed that 9.3% of
98 all cells possessed a 1n DNA content corresponding to haploid cells in G0-, G1- and S-
99 phase, which is approximately half the fraction of haploid ESCs at the beginning of
100 differentiation (16.8%; Figure 1E, F). To confirm a haploid karyotype in PGCLCs, we sorted
101 cells expressing SSEA1 and integrin β3 from d7 EBs and prepared chromosome spreads.
102 As expected, a set of 20 acrocentric chromosomes typical for an intact haploid mouse
103 genome could be observed (Figure 1G). Transcription analysis of sorted PGCLCs revealed
104 the upregulation of the PGC-markers *Blimp1*, *Prdm14*, *Tfap2c* and *Stella*, and the
105 downregulation of *Dnmt3b* in G0/G1/S-phase haploid (1n) as well as in S/G2/M-phase
106 diploid (4n) PGCLCs relative to EpiLCs and ESCs (Figure 2). These results show that
107 differentiation of haploid PGCLCs *in vitro* recapitulates gene expression changes that are
108 anticipated from the development of PGCs *in vivo*.
109

110 **PGCLCs preferentially maintain a haploid genome**

111 The PGCLC population of d7 EBs appeared to have a notably high content of haploid cells
112 (Figure 3A, B). We therefore further charcteized the percentage of PGCLCs in windows of
113 different DNA content. We analyzed the 1n population (G0/G1/S-phase haploid), the 2n
114 population (G2/M-phase haploid and G0/G1-phase diploid), and 4n population (S/G2/M-

115 phase diploid). In addition, we also analyzed the combined 2n and 4n population containing
116 all but the 1n haploid cells. PGCLCs accounted for 32.3% of 1n (G0/G1/S-phase) haploid
117 cells, while 11.1% of all cells and less than 10% of cell population with higher DNA content
118 expressed both PGC markers (Figure 3C). Therefore, the 1n haploid population contained
119 a 3-fold higher percentage of PGCLCs. The apparent enrichment of haploid cells within the
120 PGCLC population can in part be attributed to high diploidization rates that accompany
121 differentiation into somatic lineages. Nevertheless, a substantially higher percentage of
122 haploid cells was observed in PGCLCs (27.5%) compared to overall population of ESCs
123 (16.8%), EpiLCs (14.3%) and d7 EBs (9.3%; Figure 3D). These results indicate that
124 PGCLCs preferentially maintain a haploid genome.
125

126 **_Xist_ is activated from a single X chromosome in a haploid genome**

127 Germline differentiation facilitates an investigation of *Xist* expression in haploid cells
128 without caveats that arise from diploidization or cell death. We used sorted 1n (G0/G1/S-
129 phase haploid) and 4n (S/G2/M-phase diploid) cells at different timepoints for *Xist* RNA
130 FISH analysis. One and two punctate *Xist* signals were observed in haploid and diploid
131 ESCs, respectively (Figure 4A). Our analysis aimed at the detection of *Xist* clusters and
132 therefore used double stranded probes that also recognize nascent *Xist* and *Tsix* transcripts
133 before initiation of XCI as a punctate focal signal. The majority of haploid and diploid ESCs
134 showed no *Xist* cluster (Figure 4B). After the initiation of differentiation, *Xist* RNA clusters
135 were observed in 59.0% of diploid EpiLCs as expected (Wutz and Jaenisch, 2000). A clear
136 *Xist* cluster was also observed in 42.0% of sorted haploid EpiLCs indicating the initiation of
137 XCI. *Xist* is activated from the single X chromosome in haploid cells with a similar frequency

138 as from one of the two X chromosomes in diploid cells. Furthermore, 17.9% of diploid
139 EpiLCs contained two separate *Xist* clusters. This observation might be explained by
140 considering that the decision to activate *Xist* may have occurred before diploidization, when
141 the cell was in a haploid state, and *Xist* expression was maintained on both X chromosomes
142 after diploidization. Strong upregulation of *Xist* was also confirmed by quantitative RT-PCR
143 analysis in both haploid and diploid EpiLCs (Figure 2).

144 With further differentiation, we found that the proportion of cells exhibiting *Xist*
145 clusters decreased (Figure 4A, B). Only 8.7% and 24.0% of haploid and diploid d7 PGCLCs
146 showed *Xist* clusters, respectively. This observation might reflect the repression of *Xist* in
147 germ cell differentiation and cell selection that is expected from the loss of X-linked gene
148 expression in haploid cells after inactivation of the single X chromosome. The ability to
149 repress *Xist* may contribute to the ability of the germline to maintain a haploid genome with
150 a higher frequency than somatic lineages that normally do not express repressors of *Xist*.
151 Taken together, our data demonstrate that *Xist* is activated from a single X chromosome
152 without *Xic* pairing in differentiating haESCs.

153

154 # Discussion

155 Our observation that haESCs maintain a haploid genome during germ cell differentiation
156 enabled us to analyze *Xist* activation in the context of a haploid genome. Diploid mouse
157 ESCs activate *Xist* upon entering differentiation and have been used as a model for
158 studying the underlying regulation of XCI. Our results are explained by the idea that the
159 amount of blocking factors produced from a single set of autosomes is insufficient to
160 counteract activators from a single X chromosome. In contrast, X-linked activators are

161 titrated by a double dose of blocking factors in diploid male cells preventing *Xist* activation.
162 Our result therefore supports a model of diffusible X-linked activators and autosomal
163 blocking factors (Barakat et al., 2014; Pollex and Heard, 2019). We note that haploid cells
164 have a smaller cell volume than diploid cells (Freimann and Wutz, 2017), and it is not
165 entirely clear if cell volume could have an influence on XCI. Previous studies have also
166 linked the activation of *Xist* with *Xic* pairing in differentiating diploid ESCs (Bacher et al.,
167 2006; Xu et al., 2006). *Xic* pairing cannot occur in haploid cells as only a single X
168 chromosome is present. Our experiment shows that *Xist* activation does not strictly depend
169 on *Xic* pairing. This observation does not rule out that *Xic* pairing contributes to XCI in
170 diploid cells or has a role in ensuring that one X chromosome remains active after the
171 decision for initiating XCI has been taken in female cells. A recent study has reported on
172 engineering the *Xic* regions for tethering to the nuclear lamina (Pollex and Heard, 2019).
173 XCI was initiated in female mouse ESCs despite *Xic* movement was restricted.

174 Previously, *XIST* expression has been analyzed in human haESCs (Sagi et al., 2016).
175 XCI in the human embryo is regulated differently from the mouse. *XIST* is initially expressed
176 from the single and both X chromosomes in male and female embryos, respectively
177 (Okamoto et al., 2011). In contrast to mouse, *XIST* does not lead to chromosomal silencing
178 in human preimplantation embryos. The *XACT* gene, which is not present in mice, prevents
179 silencing and a partial repression of X-linked genes is observed that has been termed
180 "dampening" (Sahakyan et al., 2017). After implantation *XIST* expression becomes
181 monoallelic in female embryos and XCI is initiated. Conversely, the post implantation
182 human male embryo ceases *XIST* expression. Female human ESCs show monoallelic
183 *XIST* expression and an Xi. During culture erosion of the Xi has been observed, which is

184 characterized by a loss of *XIST* expression and reactivation of genes from the Xi to various
185 extent. Established human haESC lines have been shown to lack *XIST* expression (Sagi
186 et al., 2016). Although, this observation is expected, it is not entirely clear how an *XIST*
187 negative state was established. Lack of *XIST* activation, selection of cells with an active X
188 chromosome, and the erosion of an Xi can be considered. The fact that *XIST* is initially
189 expressed from all X chromosomes in human diploid preimplantation embryos, suggests
190 that it is also activated in haploid embryos. It is conceivable that mechanisms that prevent
191 inactivation including *XACT* could contribute to survival and potentially lead to repression
192 of *XIST* in human haESCs (Vallot et al., 2017). Irrespectively, it is likely that the lack of *XIST*
193 expression in established haESC lines does not reflect the state of the embryonic cell of
194 origin. In contrast, mouse ESCs have not initiated XCI. Capturing of the earliest stages of
195 XCI upon entry into differentiation permits the study of the X chromosome counting
196 mechanism in culture.

197 Our study also reveals that PGCLCs maintain a haploid genome with high frequency.
198 Therefore, the diploidization rate during germline differentiation is comparable to haESCs
199 and substantially lower than that of somatic lineages. PGCs have a similar epigenetic state
200 to ESCs, which might contribute to tolerance of a haploid genome. Firstly, during migration
201 to the gonads, the Xi becomes reactivated suggesting that dosage compensation is not
202 essential for germ cell development. Secondly, ESCs and PGCs exhibit genome-wide DNA
203 hypomethylation (Leitch et al., 2013). Lastly, transcription factors that are associated with
204 pluripotent cells and germ cells including Oct4 have been implicated as repressors of *Xist*
205 (Donohoe et al., 2009; Navarro et al., 2010; Nesterova et al., 2011). It is conceivable that
206 the expression of potential repressors of *Xist* in PGCs might contribute to the maintenance

207 of a haploid genome consistent with our finding that *Xist* expression is lost at later time
208 points in differentiating cultures. Oct4 is also expressed in EpiLCs and, thus, cannot explain
209 repression of *Xist* in ESCs and PGCs. However, other factors have also been implicated in
210 *Xist* repression in pluripotent cells. Haploid PGCLCs will be useful for future studies of
211 ploidy restriction and the genetics of germ cell development.
212
213
214

215 # Experimental Procedures

216 ## Derivation and culture of haESC lines

217 Derivation of haESC lines from 129S6/SvEvTac mice was performed as previously
218 described (Leeb and Wutz, 2011). At passage 5, G0/G1/S-phase haploid cell population of
219 a haESC line was purified by fluorescence-activated cell sorting (FACS) using flow
220 cytometer (MoFlo Astrios EQ, Beckman Coulter) after Hoechst 33342 (Invitrogen) staining.
221 Sorted cells were cultured and maintained on a gelatin-coated plate with irradiated mouse
222 embryonic fibroblasts (MEFs) of DR4 mouse embryos at E12.5 (The Jackson Laboratory,
223 no. 003208). Cells were maintained in Serum+2i+LIF medium, which was mixed with equal
224 volume of Serum+LIF medium without 2i (Postlmayr et al., 2020) and 2i+LIF medium
225 (Hayashi and Saitou, 2013). At passage 10, G0/G1/S-phase haploid cell population of the
226 haESC line was purified by FACS and was maintained on a gelatin-coated plate with MEFs
227 in Serum+2i+LIF medium.

228

229 ## *In vitro* germ cell differentiation

230 Germ cell differentiation was performed following a published protocol (Hayashi and Saitou,
231 2013) with a few modification. The haESC line was cultured on an ornithine- and laminin-
232 coated plate without MEFs in 2i+LIF medium from passage 12. At passage 15, EpiLC
233 differentiation was initiated as described in the protocol. After 2 days of EpiLC differentiation,
234 2.3 x 10^5 EpiLCs were plated into a well of a Sphericalplate 5D (Kugelmeiers Ltd.) with 1.4
235 ml of PGCLC differentiation medium not containing BMP8a. After 4 days of PGCLC
236 differentiation, half of the medium was replaced with fresh PGCLC differentiation medium
237 not containing BMP4 and BMP8a.

238

239 **Flow cytometry analysis and cell sorting**

240 To investigate the cell cycle of haploid and diploid cells and PGCLCs, flow cytometry
241 analysis was performed to ESCs, EpiLCs and EBs by following procedures. Cells were
242 harvested from culture vessels as described in a published protocol (Hayashi and Saitou,
243 2013), followed by staining with 15 μg/ml Hoechst 33342 for 12 min at 37 °C. Subsequently,
244 PE anti-integrin β3 (BioLegend, no. 104307) and eFluor 660 anti-SSEA1 (eBioscience, no.
245 50881341) were added to the cell suspension at concentration of 1 μg/ml and 0.12 μg/ml,
246 respectively, and the cell sample was kept on ice for 12 min. The fluorescence of each dye
247 was measured by flow cytometry. Cell cycle of haploid and diploid cells was determined
248 based on peaks of cell population at 1n and 2n DNA contents, corresponding to G0/G1-
249 phase haploid cells and G2/M-phase haploid and G0/G1-phase diploid cells, respectively,
250 by measuring the signal of Hoechst 33342. The population of PGCLCs was determined by
251 measuring the signals of PE and eFluor 660.

252

253 **Karyotyping**

254 On day 7 of germ cell differentiation, M-phase arrest of EBs was performed by culturing in
255 PGCLC differentiation medium supplemented with 0.05 mg/ml demecolcine (Merck) for 8
256 hours. Subsequently, PGCLCs were sorted by FACS. Chromosome counting of PGCLCs
257 was performed as previously described (Aizawa et al., 2020).

258

259 **Transcription analysis**

260 During germ cell differentiation of mixed haploid-diploid ESCs, G0/G1/S-phase haploid and

261 S/G2/M-phase diploid ESCs, EpiLCs and d7 PGCLCs were sorted from ESCs, EpiLCs and
262 d7 EBs by FACS, respectively. E12.5 gonads were harvested from 129S6/SvEvTac mouse
263 embryos. Sex of the gonads was determined by their morphology. PGCs were identified as
264 gonadal cells positive for both SSEA1 and integrin β3 and were sorted by FACS. RNA of
265 each sample was extracted using the RNeasy Mini Kit (Qiagen) following the
266 manufacturer's protocol, including an on-column DNA digest using RNase-free DNase
267 (Qiagen). RNA concentration was determined using a NanoDrop Lite (Thermo Fisher
268 Scientific). 100 - 500 ng total RNA was reverse transcribed using the PrimeScript RT Master
269 Mix (Takara) according to the manufacturer's instruction. RT-PCR was performed on a 384
270 well format with the 480 Lightcycler instrument (Roche) using KAPA SYBR FAST qPCR
271 KIT (Kapa Biosystems). Fold change expression was calculated using the ΔΔct method.
272 *Gapdh* expression of G0/G1/S-phase haploid ESCs was used to normalize the transcription
273 of G0/G1/S-phase EpiLCs and d7 PGCLCs. *Gapdh* expression of S/G2/M-phase diploid
274 ESCs was used to normalize the transcription of S/G2/M-phase EpiLCs, d7 PGCLCs and
275 PGCs. Primers used for transcription analysis are listed in Table S1.
276

277 ***Xist* RNA FISH**

278 RNA FISH was performed to analyze *Xist* expression during germ cell differentiation of
279 mixed haploid-diploid ESCs. FISH probe was prepared from ptetOP-Xist-PA plasmid with
280 Cy3-dCTP (Amersham Biosciences) as described previously (Wutz and Jaenisch, 2000).
281 G0/G1/S-phase haploid and S/G2/M-phase diploid ESCs, EpiLCs and d7 PGCLCs were
282 sorted by FACS, respectively. Sorted cells were mounted onto glass slides using Cytospin
283 4 (Thermo Scientific) for 3 min at 800 or 900 rpm for haploid or diploid cells, respectively.

284 Glass slides were immediately rinsed in PBS and washed in CSK buffer (100 nM NaCl, 300
285 nM sucrose, 3 mM $MgCl_2$, 10 mM PIPES pH 6.8) for 30 sec, in CSK buffer + 0.5% Triton
286 X-100 for 2 min and again in CSK buffer for 30 sec. Cells were fixed in 4%
287 paraformaldehyde in PBS for 10 min and washed in 70%, 80%, 95% and 100% EtOH for
288 2 min each. After airdrying the slides, hybridization was performed by applying probe to the
289 cells. Probes were covered with a coverslip and sealed with rubber cement. Slides were
290 then placed in a humidified chamber and incubated overnight at 37°C. Coverslips were
291 removed and slides were washed in 2X SSC + formamide (50%) for 15 min at 39°C, in 2X
292 SCC three times for 5 min each at 39°C, in 1X SSC for 10 min and in 4X SSC with a dip
293 (20X SSC: 3 M NaCl, 0.3 M tri-sodium citrate dihydrate in H_2O). Cellular DNA was
294 counterstained by incubating slides in 4X SSC + 0.1% Tween + 14 mM DAPI for 1.5 min.
295 Slides were washed with 4X SSC for 5 min. After washing, the sample was mounted in
296 Vectashield (Vector Laboratories) and covered with a coverslip. Samples were imaged
297 under the microscope (Axio Observer Z1, Zeiss) equipped with an ORCA-Flash4.0 camera
298 (Hamamatsu Photonics K.K.). Images were processed using Zeiss Zen Pro 2.0 software.
299

300 **Statistical analysis**

301 For comparison of cell population ratio (Figure 3C, D), measurements were analyzed with
302 the GraphPad Prism 8 software using a two-tailed t-test. A p-value < 0.05 was considered
303 statistically significant.
304
305

Acknowledgments

We thank Dr. Giulio Di Minin for derivation of haESC lines. This study was supported by the Swiss National Science Foundation (grant 31003A_152814/1).

Author Contributions

E.A. and A.W. conceptualized experiments. E.A., C.K., S.S. and R.F. collected the data. E.A. and C.K. analyzed the data. E.A. and A.W. wrote the manuscript.

Declaration of Interests

The authors declare no competing interests.

Supplemental Information

Table S1. List of oligos

321 # Figure Legends

322 **Figure 1. HaESCs differentiate to haploid PGCLCs by an in vitro culture.**

323 (A) A scheme of germ cell differentiation of mixed haploid-diploid ESCs. (B) Morphology of
324 ESCs, EpiLCs and d7 EBs derived from mixed haploid-diploid ESCs. Scale bar, 100 μm.
325 (C) A representative flow cytometry analysis of d7 EBs derived from mixed haploid-diploid
326 ESCs. PGCLCs, positive for both SSEA1 and integrin β3, accounted for 15.1% out of all
327 cells. (D, E) The proportion of PGCLCs (D) and G0/G1/S-phase haploid cells (E) out of all
328 cells at the different stages during germ cell differentiation of mixed haploid-diploid ESCs.
329 n = 14 (ESC), 9 (EpiLC), 7 (d6 EB), 18 (d7 EB) and 7 (d8 EB). Data represents the mean
330 value and the standard error of the mean. (F) Flow cytometry analysis of DNA content of
331 diploid ESCs, mixed haploid-diploid ESCs, and d7 EBs derived from mixed haploid-diploid
332 ESCs. Cell cycle phases of haploid and diploid cells (top), and PGCLCs in d7 EBs (green)
333 are indicated. (G) Representative chromosome spread of a haploid d7 PGCLC.

334

335 **Figure 2. Transcription profile of haploid and diploid cells during germ cell**
336 **differentiation *in vitro*.**

337 Transcription of PGC markers (*Blimp1*, *Prdm14*, *Tfap2c* and *Stella*), *Dnmt3b* and *Xist*
338 during germ cell differentiation of mixed haploid-diploid ESCs. Gene expression of
339 G0/G1/S-phase haploid and S/G2/M-phase diploid cells of ESCs, EpiLCs and d7 EBs was
340 measured, respectively. Female and male PGCs purified from E12.5 gonads by FACS were
341 used as controls. Gene expression of G0/G1/S-phase haploid and S/G2/M-phase diploid
342 samples was normalized to *Gapdh* expression relative to G0/G1/S-phase haploid and
343 S/G2/M-phase diploid ESCs, respectively. Gene expression of male and female PGCs was

344 normalized to *Gapdh* expression relative to S/G2/M-phase diploid ESCs. Data represents
345 relative expression of each sample with the mean value and the standard error of the mean
346 (n = 4). H, G0/G1/S-phase haploid; D, S/G2/M-phase diploid; F, female; M, male.
347

348 **Figure 3. PGCLCs preferentially maintain haploidy *in vitro*.**

349 (A) A representative distribution of DNA content in d7 EBs derived from mixed haploid-
350 diploid ESCs. PGCLCs, positive for SSEA1 and integrin β3, are indicated by green color.
351 The cell cycle profile of haploid and diploid cells is shown at the top. (B) A representative
352 flow cytometry analysis of d7 EBs. PGCLCs accounted for 11.2% out of all cells in d7 EBs
353 derived from mixed haploid-diploid ESCs. PGCLCs accounted for 38.1%, 9.2%, 6.3% and
354 8.7% out of G0/G1/S haploid cell population, G2/M haploid + G0/G1 diploid cell population,
355 S/G2/M diploid cell population, and G2/M haploid + all diploid cell population of d7 EBs
356 derived from mixed haploid-diploid ESCs, respectively. Embryonic female gonads at E12.5
357 and d7 EBs derived from diploid ESCs were also analyzed as controls. (C) The ratio of
358 PGCLCs in cell populations of different DNA content in d7 EBs derived from mixed haploid-
359 diploid ESCs or diploid ESCs. PGCLCs accounted for 32.3% on average out of G0/G1/S
360 haploid cells in d7 EBs derived from mixed haploid-diploid ESCs. Data represents the mean
361 and the standard error of the mean. n = 18 (d7 EBs derived from mixed haploid-diploid
362 ESCs) and n = 12 (d7 EBs derived from diploid ESCs). **** $P < 0.0001$. (D) Cell cycle
363 distribution of haploid and diploid cells during germ cell differentiation of mixed haploid-
364 diploid ESCs. Data represents the mean value and the standard error of the mean. n = 14
365 (ESC), 9 (EpiLC), 18 (d7 EB) and 18 (d7 PGCLC). **** $P < 0.0001$.
366

367 **Figure 4. *Xist* is activated and repressed in both haploid and diploid cells**
368 **during germ cell differentiation.**

369 (A) Representative images of *Xist* expression during germ cell differentiation of mixed
370 haploid-diploid ESCs detected by RNA FISH using a Cy3-labeled *Xist* probe (orange). No
371 *Xist* cluster but single foci observed in G0/G1/S-phase haploid ESCs and PGCLCs. No
372 cluster but double foci observed in S/G2/M-phase diploid ESCs and PGCLCs. Single *Xist*
373 clusters (arrow) and foci (arrowhead) observed in G0/G1/S-phase haploid EpiLCs. Double
374 clusters (asterisk), single clusters (arrow) and no cluster (arrowhead) observed in each
375 S/G2/M-phase diploid EpiLC. (B) Proportion of *Xist* RNA FISH signals during germ cell
376 differentiation of mixed haploid-diploid ESCs. The number of cells possessing no, single or
377 double *Xist* RNA clusters were counted in G0/G1/S-phase haploid and S/G2/M-diploid cells.
378 Total numbers of counted cells are 138 (H, ESC), 171 (D, ESC), 100 (H, EpiLC), 173 (D,
379 EpiLC), 69 (H, PGCLC) and 121 (D, PGCLC). D, S/G2/M-phase diploid; H, G0/G1/S-phase
380 haploid.

381

382 # References

383 Aizawa, E., Dumeau, C.-E., Freimann, R., Di Minin, G., and Wutz, A. (2020). Polyploidy of semi-cloned embryos
384 generated from parthenogenetic haploid embryonic stem cells. PLOS ONE *15*, e0233072.
385 Augui, S., Filion, G.J., Huart, S., Nora, E., Guggiari, M., Maresca, M., Stewart, A.F., and Heard, E. (2007). Sensing
386 X chromosome pairs before X inactivation via a novel X-pairing region of the Xic. Science (New York, NY) *318*,
387 1632-1636.
388 Bacher, C.P., Guggiari, M., Brors, B., Augui, S., Clerc, P., Avner, P., Eils, R., and Heard, E. (2006). Transient
389 colocalization of X-inactivation centres accompanies the initiation of X inactivation. Nature cell biology *8*,
390 293-299.
391 Barakat, T.S., Loos, F., van Staveren, S., Myronova, E., Ghazvini, M., Grootegoed, J.A., and Gribnau, J. (2014).
392 The trans-activator RNF12 and cis-acting elements effectuate X chromosome inactivation independent of X-
393 pairing. Molecular cell *53*, 965-978.
394 Donohoe, M.E., Silva, S.S., Pinter, S.F., Xu, N., and Lee, J.T. (2009). The pluripotency factor Oct4 interacts with
395 Ctcf and also controls X-chromosome pairing and counting. Nature *460*, 128-132.
396 Elling, U., Taubenschmid, J., Wirnsberger, G., O'Malley, R., Demers, S.P., Vanhaelen, Q., Shukalyuk, A.I.,
397 Schmauss, G., Schramek, D., Schnuetgen, F.*, et al.* (2011). Forward and reverse genetics through derivation

398 of haploid mouse embryonic stem cells. Cell Stem Cell *9*, 563-574.
399 Freimann, R., and Wutz, A. (2017). A fast and efficient size separation method for haploid embryonic stem
400 cells. Biomicrofluidics *11*, 054117.
401 Galupa, R., and Heard, E. (2018). X-Chromosome Inactivation: A Crossroads Between Chromosome
402 Architecture and Gene Regulation. Annual review of genetics *52*, 535-566.
403 Hayashi, K., Ogushi, S., Kurimoto, K., Shimamoto, S., Ohta, H., and Saitou, M. (2012). Offspring from oocytes
404 derived from in vitro primordial germ cell-like cells in mice. Science (New York, NY) *338*, 971-975.
405 Hayashi, K., Ohta, H., Kurimoto, K., Aramaki, S., and Saitou, M. (2011). Reconstitution of the mouse germ cell
406 specification pathway in culture by pluripotent stem cells. Cell *146*, 519-532.
407 Hayashi, K., and Saitou, M. (2013). Generation of eggs from mouse embryonic stem cells and induced
408 pluripotent stem cells. Nat Protoc *8*, 1513-1524.
409 He, W., Zhang, X., Zhang, Y., Zheng, W., Xiong, Z., Hu, X., Wang, M., Zhang, L., Zhao, K., Qiao, Z.*, et al.* (2018).
410 Reduced Self-Diploidization and Improved Survival of Semi-cloned Mice Produced from Androgenetic Haploid
411 Embryonic Stem Cells through Overexpression of Dnmt3b. Stem cell reports *10*, 477-493.
412 He, Z.Q., Xia, B.L., Wang, Y.K., Li, J., Feng, G.H., Zhang, L.L., Li, Y.H., Wan, H.F., Li, T.D., Xu, K.*, et al.* (2017).
413 Generation of Mouse Haploid Somatic Cells by Small Molecules for Genome-wide Genetic Screening. Cell Rep
414 *20*, 2227-2237.
415 Hill, P.W.S., Leitch, H.G., Requena, C.E., Sun, Z., Amouroux, R., Roman-Trufero, M., Borkowska, M., Terragni, J.,
416 Vaisvila, R., Linnett, S.*, et al.* (2018). Epigenetic reprogramming enables the transition from primordial germ
417 cell to gonocyte. Nature *555*, 392-396.
418 Kay, G.F., Penny, G.D., Patel, D., Ashworth, A., Brockdorff, N., and Rastan, S. (1993). Expression of Xist during
419 mouse development suggests a role in the initiation of X chromosome inactivation. Cell *72*, 171-182.
420 Leeb, M., Walker, R., Mansfield, B., Nichols, J., Smith, A., and Wutz, A. (2012). Germline potential of
421 parthenogenetic haploid mouse embryonic stem cells. Development (Cambridge, England) *139*, 3301-3305.
422 Leeb, M., and Wutz, A. (2011). Derivation of haploid embryonic stem cells from mouse embryos. Nature *479*,
423 131-134.
424 Leitch, H.G., McEwen, K.R., Turp, A., Encheva, V., Carroll, T., Grabole, N., Mansfield, W., Nashun, B., Knezovich,
425 J.G., Smith, A.*, et al.* (2013). Naive pluripotency is associated with global DNA hypomethylation. Nature
426 structural & molecular biology *20*, 311-316.
427 Lyon, M.F. (1961). Gene Action in the X-chromosome of the Mouse (Mus musculus L.). Nature *190*, 372-373.
428 Mak, W., Nesterova, T.B., de Napoles, M., Appanah, R., Yamanaka, S., Otte, A.P., and Brockdorff, N. (2004).
429 Reactivation of the paternal X chromosome in early mouse embryos. Science (New York, NY) *303*, 666-669.
430 Monkhorst, K., Jonkers, I., Rentmeester, E., Grosveld, F., and Gribnau, J. (2008). X inactivation counting and
431 choice is a stochastic process: evidence for involvement of an X-linked activator. Cell *132*, 410-421.
432 Navarro, P., Oldfield, A., Legoupi, J., Festuccia, N., Dubois, A., Attia, M., Schoorlemmer, J., Rougeulle, C.,
433 Chambers, I., and Avner, P. (2010). Molecular coupling of Tsix regulation and pluripotency. Nature *468*, 457-
434 460.
435 Nesterova, T.B., Senner, C.E., Schneider, J., Alcayna-Stevens, T., Tattermusch, A., Hemberger, M., and
436 Brockdorff, N. (2011). Pluripotency factor binding and Tsix expression act synergistically to repress Xist in
437 undifferentiated embryonic stem cells. Epigenetics & chromatin *4*, 17.
438 Ohhata, T., and Wutz, A. (2013). Reactivation of the inactive X chromosome in development and
439 reprogramming. Cellular and molecular life sciences : CMLS *70*, 2443-2461.
440 Ohinata, Y., Ohta, H., Shigeta, M., Yamanaka, K., Wakayama, T., and Saitou, M. (2009). A signaling principle
441 for the specification of the germ cell lineage in mice. Cell *137*, 571-584.
442 Okamoto, I., Otte, A.P., Allis, C.D., Reinberg, D., and Heard, E. (2004). Epigenetic dynamics of imprinted X
443 inactivation during early mouse development. Science (New York, NY) *303*, 644-649.
444 Okamoto, I., Patrat, C., Thepot, D., Peynot, N., Fauque, P., Daniel, N., Diabangouaya, P., Wolf, J.P., Renard, J.P.,

445 Duranthon, V*., et al.* (2011). Eutherian mammals use diverse strategies to initiate X-chromosome inactivation
446 during development. Nature *472*, 370-374.
447 Olbrich, T., Mayor-Ruiz, C., Vega-Sendino, M., Gomez, C., Ortega, S., Ruiz, S., and Fernandez-Capetillo, O.
448 (2017). A p53-dependent response limits the viability of mammalian haploid cells. Proceedings of the
449 National Academy of Sciences of the United States of America *114*, 9367-9372.
450 Olbrich, T., Vega-Sendino, M., Murga, M., de Carcer, G., Malumbres, M., Ortega, S., Ruiz, S., and Fernandez-
451 Capetillo, O. (2019). A Chemical Screen Identifies Compounds Capable of Selecting for Haploidy in
452 Mammalian Cells. Cell Rep *28*, 597-604 e594.
453 Pollex, T., and Heard, E. (2019). Nuclear positioning and pairing of X-chromosome inactivation centers are not
454 primary determinants during initiation of random X-inactivation. Nature genetics *51*, 285-295.
455 Postlmayr, A., Dumeau, C.E., and Wutz, A. (2020). Cdk8 is required for establishment of H3K27me3 and gene
456 repression by Xist and mouse development. Development (Cambridge, England) *147*.
457 Sagi, I., Chia, G., Golan-Lev, T., Peretz, M., Weissbein, U., Sui, L., Sauer, M.V., Yanuka, O., Egli, D., and Benvenisty,
458 N. (2016). Derivation and differentiation of haploid human embryonic stem cells. Nature *532*, 107-111.
459 Sahakyan, A., Kim, R., Chronis, C., Sabri, S., Bonora, G., Theunissen, T.W., Kuoy, E., Langerman, J., Clark, A.T.,
460 Jaenisch, R*., et al.* (2017). Human Naive Pluripotent Stem Cells Model X Chromosome Dampening and X
461 Inactivation. Cell Stem Cell *20*, 87-101.
462 Sugimoto, M., and Abe, K. (2007). X chromosome reactivation initiates in nascent primordial germ cells in
463 mice. PLoS genetics *3*, e116.
464 Takagi, N., and Sasaki, M. (1975). Preferential inactivation of the paternally derived X chromosome in the
465 extraembryonic membranes of the mouse. Nature *256*, 640-642.
466 Takahashi, S., Lee, J., Kohda, T., Matsuzawa, A., Kawasumi, M., Kanai-Azuma, M., Kaneko-Ishino, T., and Ishino,
467 F. (2014). Induction of the G2/M transition stabilizes haploid embryonic stem cells. Development (Cambridge,
468 England) *141*, 3842-3847.
469 Vallot, C., Patrat, C., Collier, A.J., Huret, C., Casanova, M., Liyakat Ali, T.M., Tosolini, M., Frydman, N., Heard,
470 E., Rugg-Gunn, P.J*., et al.* (2017). XACT Noncoding RNA Competes with XIST in the Control of X Chromosome
471 Activity during Human Early Development. Cell Stem Cell *20*, 102-111.
472 Wutz, A., and Jaenisch, R. (2000). A shift from reversible to irreversible X inactivation is triggered during ES
473 cell differentiation. Molecular cell *5*, 695-705.
474 Xu, N., Donohoe, M.E., Silva, S.S., and Lee, J.T. (2007). Evidence that homologous X-chromosome pairing
475 requires transcription and Ctcf protein. Nature genetics *39*, 1390-1396.
476 Xu, N., Tsai, C.L., and Lee, J.T. (2006). Transient homologous chromosome pairing marks the onset of X
477 inactivation. Science (New York, NY) *311*, 1149-1152.
478
479

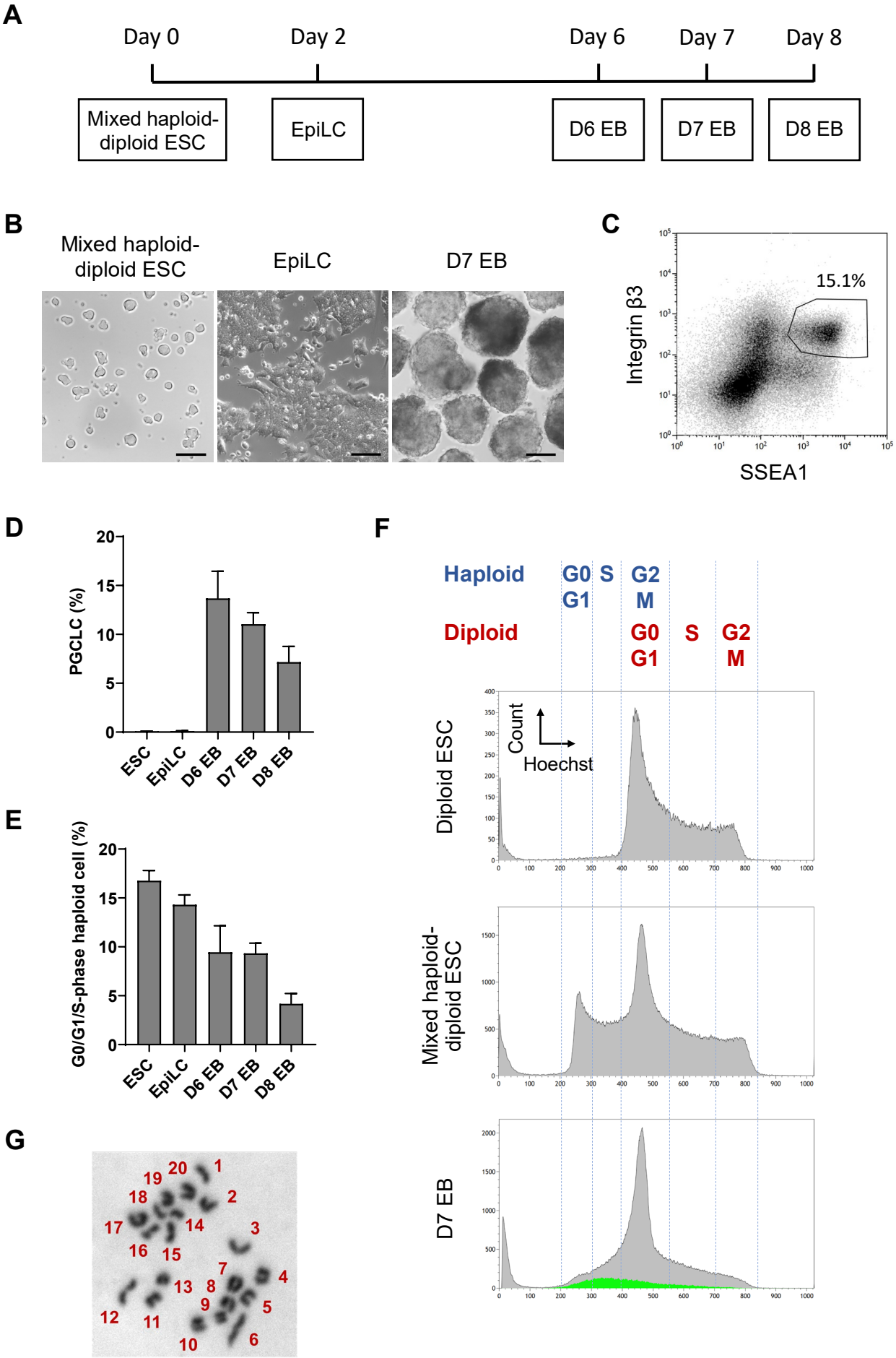
A
Day 0
Day 2
Day 6
Day 7
Day 8
Mixed haploid-diploid ESC
EpiLC
D6 EB
D7 EB
D8 EB
B
Mixed haploid-diploid ESC
EpiLC
D7 EB
C
15.1%
Integrin β3
SSEA1
D
PGCLC (%)
ESC
EpiLC
D6 EB
D7 EB
D8 EB
E
G0/G1/S-phase haploid cell (%)
ESC
EpiLC
D6 EB
D7 EB
D8 EB
F
Haploid
G0
G1
S
G2
M
Diploid
G0
G1
S
G2
M
Count
Hoechst
Diploid ESC
Mixed haploid-diploid ESC
D7 EB
G

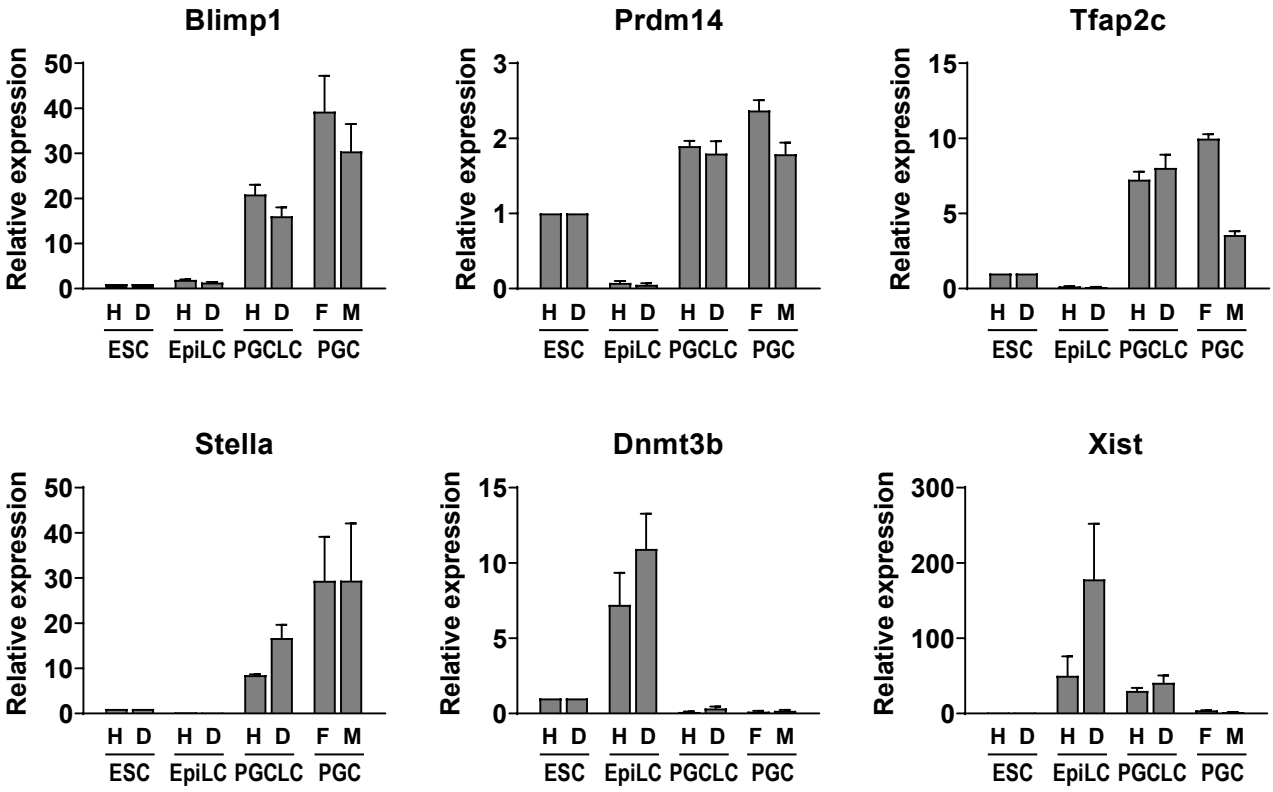
Blimp1
Prdm14
Tfap2c
Stella
Dnmt3b
Xist
Relative expression
H D H D H D F M
ESC EpiLC PGCLC PGC

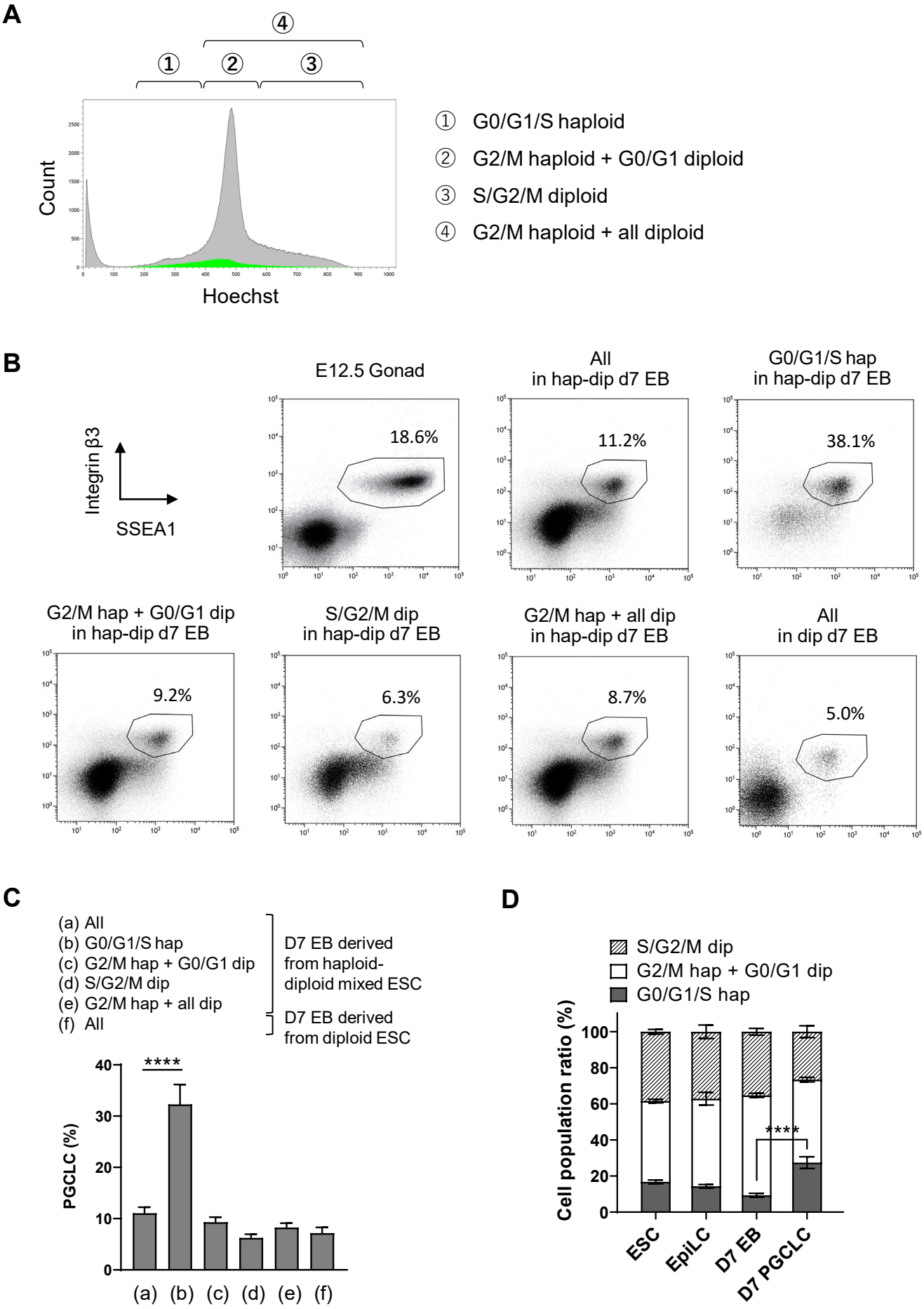
A
①
②
③
④
Count
Hoechst
① G0/G1/S haploid
② G2/M haploid + G0/G1 diploid
③ S/G2/M diploid
④ G2/M haploid + all diploid
B
Integrin β3
SSEA1
E12.5 Gonad
18.6%
All
in hap-dip d7 EB
11.2%
G0/G1/S hap
in hap-dip d7 EB
38.1%
G2/M hap + G0/G1 dip
in hap-dip d7 EB
9.2%
S/G2/M dip
in hap-dip d7 EB
6.3%
G2/M hap + all dip
in hap-dip d7 EB
8.7%
All
in dip d7 EB
5.0%
C
(a) All
(b) G0/G1/S hap
(c) G2/M hap + G0/G1 dip
(d) S/G2/M dip
(e) G2/M hap + all dip
(f) All
D7 EB derived from haploid-diploid mixed ESC
D7 EB derived from diploid ESC
****
PGCLC (%)
(a) (b) (c) (d) (e) (f)
D
S/G2/M dip
G2/M hap + G0/G1 dip
G0/G1/S hap
Cell population ratio (%)
****
ESC
EpiLC
D7 EB
D7 PGCLC

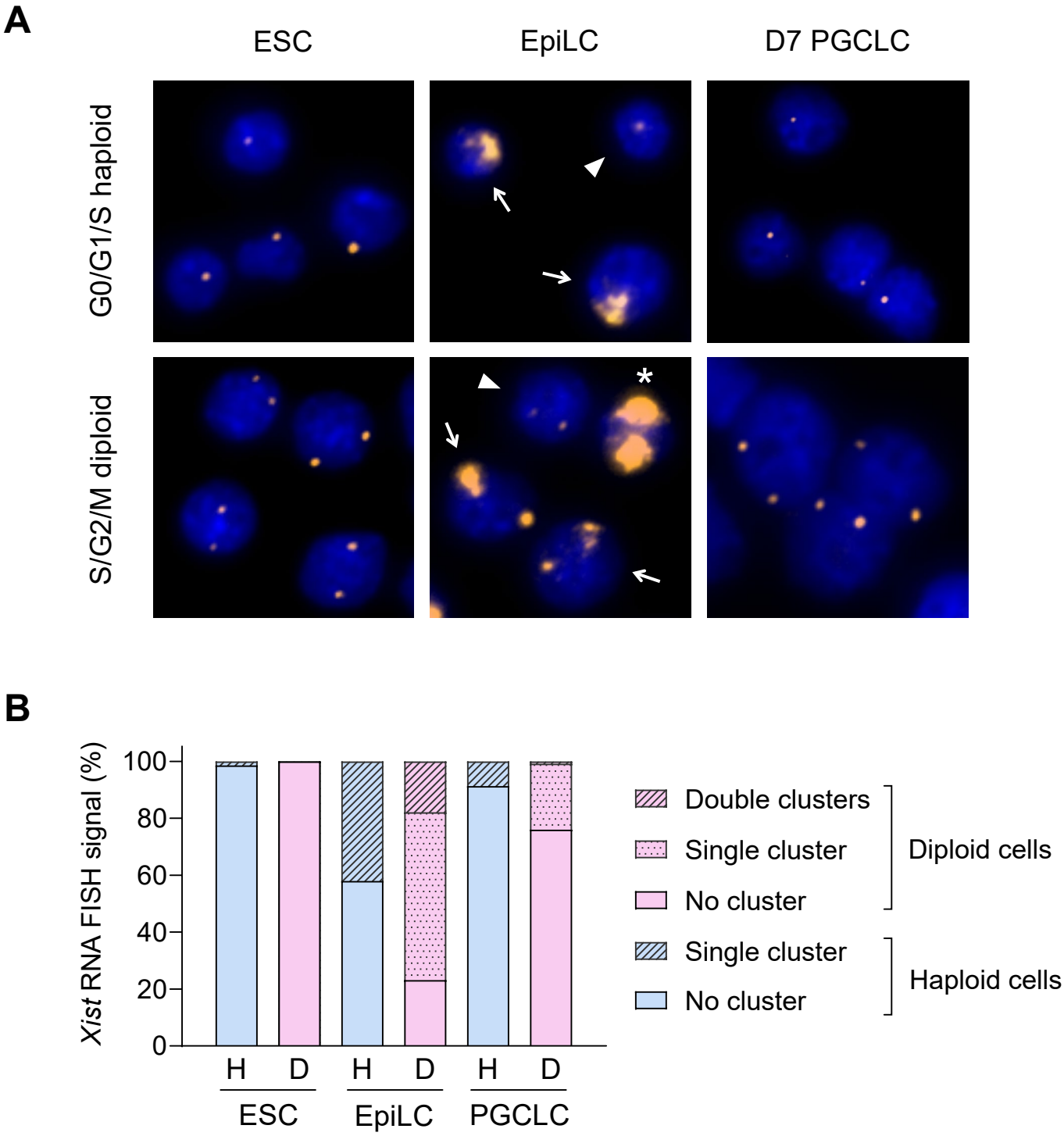
A
ESC
EpiLC
D7 PGCLC
G0/G1/S haploid
S/G2/M diploid
B
Xist RNA FISH signal (%)
100
80
60
40
20
0
H
D
H
D
H
D
ESC
EpiLC
PGCLC
Double clusters
Single cluster
No cluster
Diploid cells
Single cluster
No cluster
Haploid cells

Table S1. List of oligos

Name	Sequence (5' to 3')
Blimp1-F	AGC ATG ACC TGA CAT TGA CAC C
Blimp1-R	CTC AAC ACT CTC ATG TAA GAG GC
Dnmt3b-F	CTC GCA AGG TGT GGG CTT TTG TAAC
Dnmt3b-R	CTG GGC ATC TGT CAT CTT TGC ACC
Gapdh-1	AGG TCG GTG TGA ACG GAT TTG
Gapdh-2	TGT AGA CCA TGT AGT TGA GGT CA
Prdm14-F	ACA GCC AAG CAA TTT GCA CTA C
Prdm14-R	TTA CCT GGC ATT TTC ATT GCT C
Stella-F	AGG CTC GAA GGA AAT GAG TTT G
Stella-R	TCC TAA TTC TTC CCG ATT TTC G
Tfap2c-F	GGG CTT TTC TCT CTT GGC TGG T
Tfap2c-R	TCC ACA CGT CAC CCA CAC AA
Xist-F	GCT GGT TCG TCT ATC TTG TGG GTC
Xist-R	TTG TTC AGA GTA GCG AGG ACT TGA AGA G